Coastal flood hazard and risk maps for the Adriatic and Ionian region IT developed

D.3.2.2

Deliverable title:	Coastal flood hazard and risk maps for the Adriatic and Ionian region IT developed
Deliverable number:	D.3.2.2
Deliverable authors:	Christian Ferrarin (CNR-ISMAR), Amedeo Fadini (CNR-ISMAR)
Date release:	2023-02-15
Submitted by:	CNR-ISMAR

TABLE OF CONTENTS

1 Introduction **4**

2 The modelling system **4**

2.1 The hydrodynamic model SHYFEM 4

2.2 The wave model WWMII 5

2.3 Model setup 5

3 Model assessment **7**

3.1 Sea level validation 8

3.2 Wave validation 10

4 Adriatic Sea climatology **12**

4.1 Sea level climate 12

4.2 Significant wave height climate 15

5 Coastal flood hazard **18**

6 References **20**

1 INTRODUCTION

The STREAM project deals with territorial challenges connected to flooding in the Adriatic region. In this context, numerical modelling has become a fundamental tool for describing the dynamics of hazardous marine conditions which determine coastal flooding. The simulation results were first validated against data acquired in several in-situ observing stations. Numerical models have been here used to reproduce past sea conditions (1994-2019) in order to develop climatological flood hazard maps showing areas which could be potentially flooded.

2 THE MODELLING SYSTEM

In this study we used a coupled hydrodynamic-wave model to simulate past sea conditions in the whole Mediterranean Sea. The different modules use the same computational grid for all the processes. The application of triangular unstructured grids in both the hydrodynamic and wave models has the advantage of describing more accurately complicated bathymetry and irregular boundaries in shallow water areas. It can also solve the combined large-scale oceanic and small-scale coastal dynamics in the same discrete domain by subdivision the basin into triangles varying in form and size. The coupled SHYFEM-WWM model has already been applied to the Mediterranean and Adriatic Sea (Roland et al., 2009; Ferrarin et al., 2013);

The considered interactions between waves, surge and tides are: (1) the contribution of waves to the total water levels by means of the wave set-up and wave set-down; (2) the influence of tides and storm surge on the wave propagation affecting the refraction, shoaling and breaking processes; (3) the effect of water level variation and currents on the propagation, generation and decay of the wind waves; (4) the effect of the wave on the surface roughness and therefore on the wind drag.

2.1 The hydrodynamic model SHYFEM

The modelling framework here applied is based on the System of HydrodYnamic Finite Element Modules (SHYFEM, Umgiesser et al., 2014) code, an open-source unstructured ocean model for simulating hydrodynamics and transport processes at very high resolution. The model solves the shallow-water equations in their formulations with levels and transports using a finite element numerical method and semi-implicit time stepping. The model has been already applied to

simulate hydrodynamics in the Mediterranean Sea (Ferrarin et al., 2013; Ferrarin et al., 2018), in the Adriatic Sea (Bellafiore et al., 2018; Bajo et al., 2019; Ferrarin et al., 2019; Ferrarin et al., 2021), and in several coastal systems (see Umgiesser et al., 2014 and references therein). In this application we used a two-dimensional barotropic formulation, allowing the velocity advection.

The coupling of wave and current models was achieved through the gradients of the radiation stress induced by waves computed using the theory of Longuet-Higgins and Steward (1964). The vertical variation of the radiation stress was computed following the theory of Xia et al. (2004). The shear component of this momentum flux and the pressure gradient creates second-order currents. The model calculates equilibrium tidal potential and load tides and uses these to force the free surface (Kantha, 1995). Four semi-diurnal (M_2, S_2, N_2, K_2), four diurnal (K_1, O_1, P_1, Q_1) and four long-term constituents (Mf, Mm, Ssa, MSm) are considered by the hydrodynamic model. This study does not consider the density effects in the hydrodynamic model, and therefore on the simulated sea levels.

2.2 The wave model WWMII

WWMII is a third-generation spectral wind wave model, which uses triangular elements in geographical space to solve the Wave Action Equation (WAE) (Roland et al., 2009). The WAE describes the evolution of wind waves in slowly varying media. In this work, the wave model is coupled to the hydrodynamic model to account for wave refraction and shoaling induced by variable depths and currents.

The source term includes the energy input due to wind, the non-linear interaction in deep and shallow water, the energy dissipation due to whitecapping and depth-induced wave breaking and the energy dissipation due to bottom friction. In this study, we have adopted 32 wave frequencies, with an optimal distribution in spectral space ranging from 0.07 to 1.34 Hz, and 36 uniformly wave-distributed directions (10 deg bins).

2.3 Model setup

The hydrodynamic and wave numerical computation is performed on a spatial domain that represents the Mediterranean Sea by means of an unstructured grid. The use of elements of variable sizes, typical of finite element methods, is fully exploited, in order to suit the complicated geometry of the basin, the rapidly varying topographic features, and the complex bathymetry. The numerical grid used by the hydrodynamic and the wave model covers the whole Mediterranean

Sea with approximately 163,000 triangular elements and a resolution that varies from 8 km in the open sea to about 1 km in the coastal waters (Fig. 1).

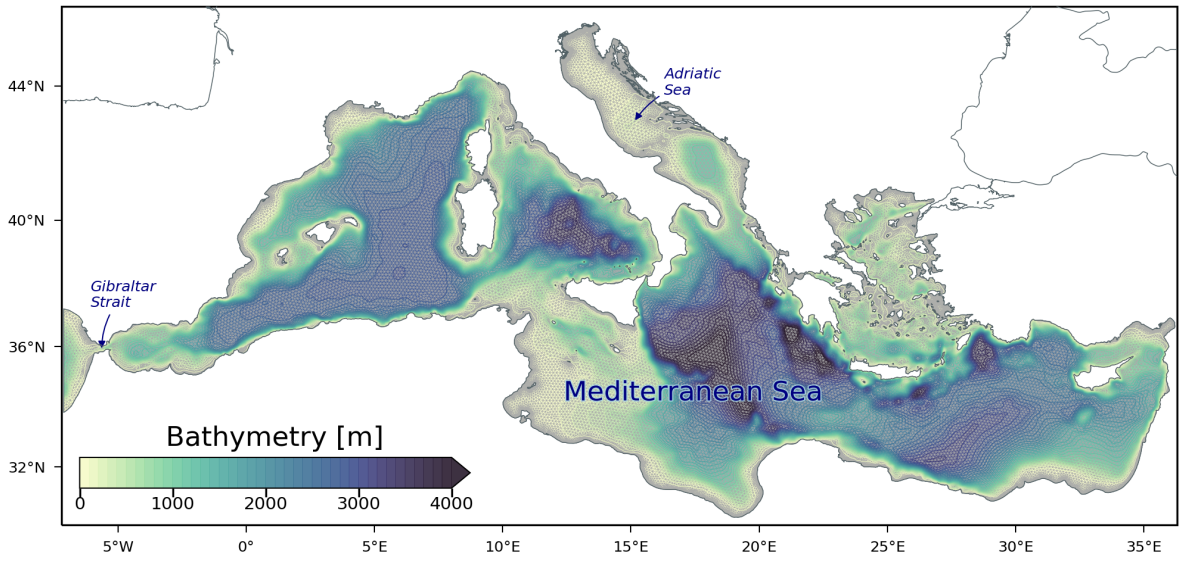

Fig. 1. Numerical grid and bathymetry of the hydrodynamic and wave models

The model bathymetry over the Mediterranean Sea is obtained by a bilinear interpolation on the model grid of the European Marine Observation and Data Network dataset (http://www.emodnet-bathymetry.eu, EMODnet 2020).

In order to reproduce the past sea conditions over the period 1994-2019, the ocean simulations were forced by the meteorological Copernicus European Regional ReAnalysis (CERRA) fields (Schimanke et al., 2021). CERRA is fully operational and is used to produce a pan-European reanalysis dataset with very high horizontal resolution (5.5 km) forced by the ERA5 global reanalysis (Hersbach et al., 2020). The added value of the CERRA data with respect to the ERA5 global reanalysis product is expected to come, for example, with the higher horizontal resolution that permits the usage of a better description of the model topography and physiographic data, and the assimilation of more surface observations. CERRA reanalysis data are available from the Copernicus Climate Data Store (https://cds.climate.copernicus.eu/). The hydrodynamic simulations were forced at the lateral boundary of the Atlantic Ocean (off the Gibraltar Strait) with the sea surface height above the geoid from the Atlantic-Iberian Biscay Irish Ocean Physics Reanalysis (Sotillo et al., 2015) made available via the Copernicus Marine Service (https://marine.copernicus.eu/).

3 MODEL ASSESSMENT

The accuracy of the model is evaluated by comparing the simulated water level and significant wave height with observations collected at different locations in the Adriatic Sea. In this work, we consider the root mean square error of the simulated values with respect to the observations (RMSE), the difference between the mean of simulation results and observations (BIAS), the Pearson cross-correlation coefficient between model results and observations (CC) and the slope of the linear regression best-fit line (SLOPE) as the metrics for measuring the accuracy of the numerical results in representing the sea level and wave variability.

In this work, the model performance was evaluated by comparison of the available sea levels recorded at 9 tide gauges station and significant wave heights recorded at 9 stations (Fig. 2).

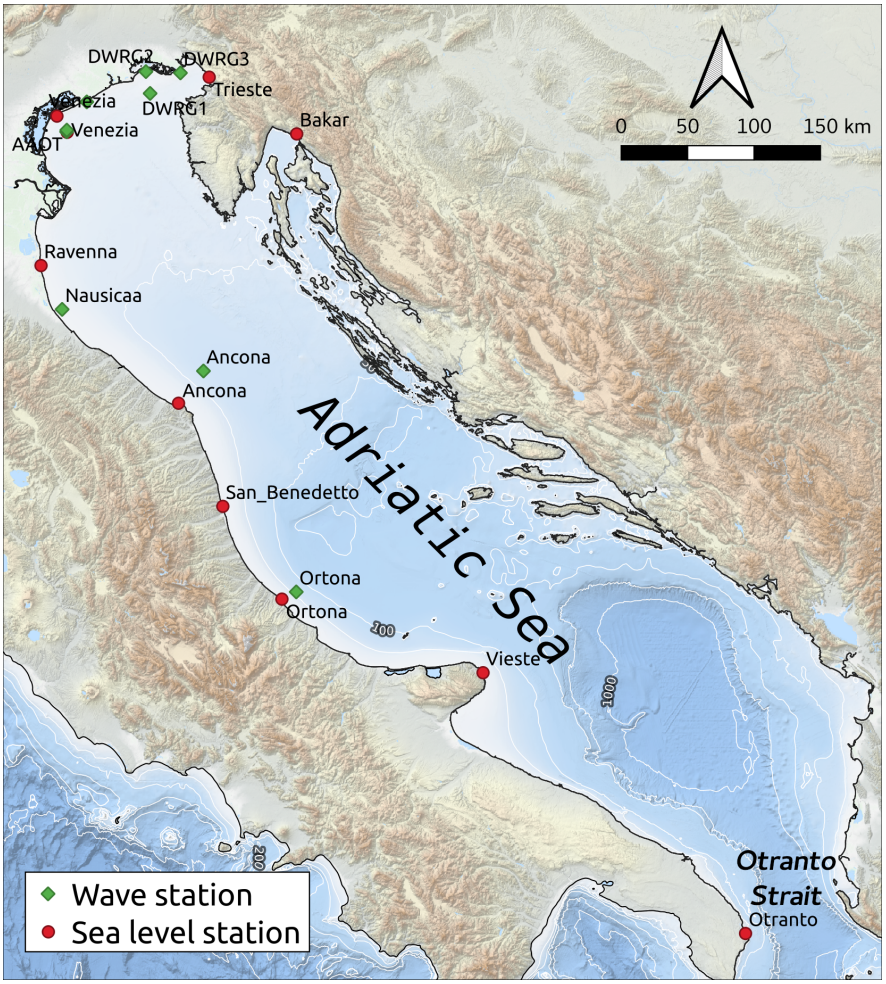

Fig. 2. Bathymetry of the Adriatic Sea with monitoring stations for sea levels (red dots) and waves (green diamonds).

3.1 Sea level validation

According to the validation results, the modelling system is capable of producing accurate simulations of the sea levels in the Adriatic Sea. Model results were extracted at the monitoring stations indicated with red dots in Fig. 2. The results of the statistical analysis of the simulated sea level are reported in Table 1 and presented in Fig. 3.

The simulated water level has a correlation higher than 0.8 (excluding Otranto) and an RMSE varying from 8 to 16 cm. Model skill is spatially varying over the considered domain. In the northern Adriatic Sea (stations of Bakar, Trieste, AAOT, Venezia and Ravenna) the model presents the best agreement with the observations, with a correlation coefficient exceeding 0.86. These stations show the highest correlations and the lowest normalized RMSE (divided by the amplitude of the variation of the observations) because the northern Adriatic Sea is characterized by the highest water level oscillations. Indeed, the contribution of the tidal signal relative to the water level variance is more than 73% in the northern Adriatic Sea, while is about 30% in its southern part. The model is slightly overestimating the highest percentiles in the northern Adriatic Sea.

Table 1. Statistical analysis of modelled water level in terms of RMSE, CC and SLOPE at the monitoring stations indicated with red dots in Fig. 2. Unit for RMSE is cm. The BIAS is not reported due to the fact that the different monitoring stations may have different reference datum.

Stations	RMSE	CC	SLOPE
Bakar	12	0.86	1.09
Trieste	16	0.88	0.96
Venezia	15	0.89	0.98
AAOT	12	0.92	1.04
Ravenna	12	0.90	1.04
Ancona	10	0.88	1.07
Ortona	9	0.84	0.99
Vieste	9	0.84	0.95
Otranto	8	0.76	0.87

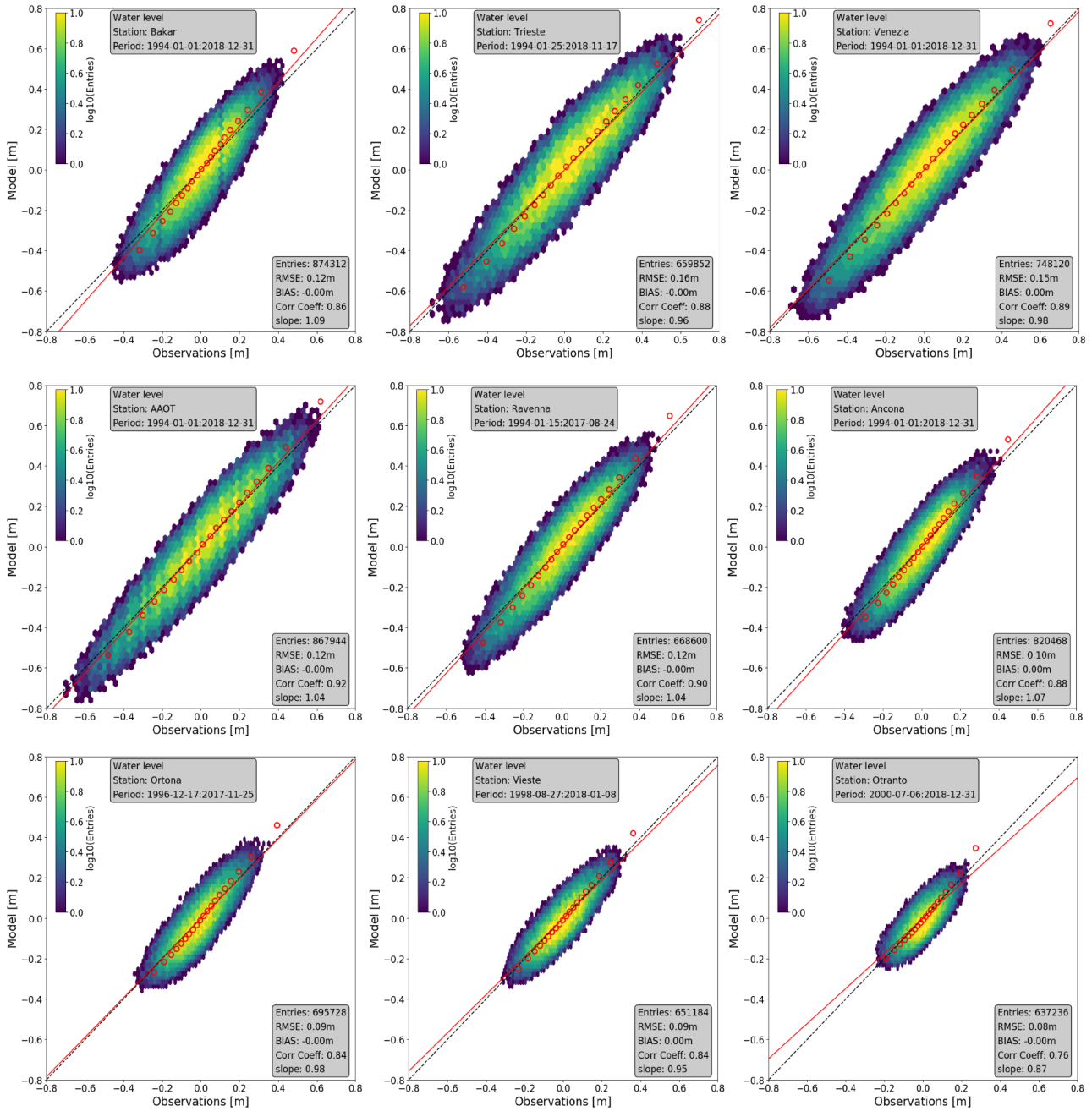

Fig. 3. Scatter plot for the water level at the different monitoring stations. Red circles are the Q-Q plot up to the 99th percentile.

3.2 Wave validation

According to the validation results, the modelling system is capable of producing accurate simulations of the wave field in the Adriatic Sea. Model results were extracted at the monitoring stations indicated with green diamonds in Fig. 2. The results of the statistical analysis of the simulated significant wave height Hs are reported in Table 2 and presented in Fig. 4.

The model results compare reasonably well with the measurements: the root mean square error (RMSE) ranges from 13 to 29 cm for the significant wave height and the correlation coefficient is always higher than 0.8. The statistical results show a small underestimation of the largest waves in the Adriatic Sea. This discrepancy could be partially due to the underestimation of the wind fields over the northern Adriatic Sea (Barbariol et al., 2021). Wave model performance is comparable with other existing wave modelling systems in the Adriatic Sea (Bertotti and Cavaleri, 2009; Barbariol et al., 2021).

Table 2. Statistical analysis of modelled significant wave height in terms of RMSE, BIAS, CC and SLOPE at the monitoring stations indicated with green diamonds in Fig. 2. Unit for RMSE e BIAS is cm.

Stations	RMSE	BIAS	CC	SLOPE
DWRG1	17	7	0.88	1.04
DWRG2	13	4	0.83	0.95
DWRG3	13	4	0.81	0.95
AW01_AWAC	13	0	0.88	0.88
AAOT	22	0	0.85	0.88
Venice	17	0	0.89	0.90
Nausicaa	15	1	0.89	0.90
Ancona	21	-2	0.93	0.98
Ortona	29	-5	0.96	0.90

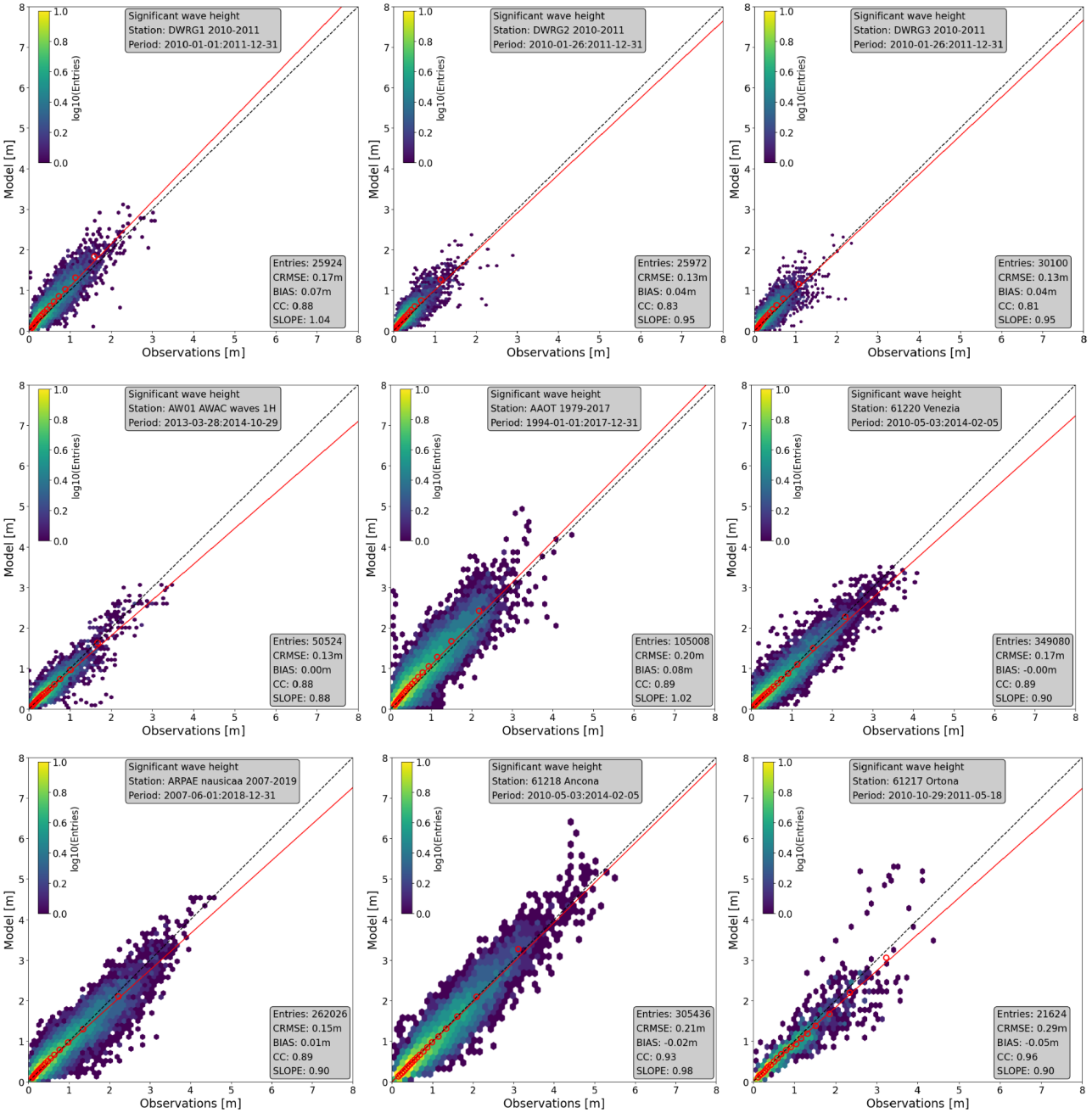

Fig. 4. Scatter plot for the significant wave height at the different monitoring stations. Red circles are the Q-Q plot up to the 99th percentile.

4 ADRIATIC SEA CLIMATOLOGY

In this section, we characterize the long-term sea level and wind-wave climate of the Adriatic Sea. The climatology of sea levels and wind-wave sea states is presented by using the 50th (i.e., median) and the 99th percentiles of the water levels and significant wave height (Hs), which may represent typical and extreme conditions, respectively. In order to highlight the effects of intra-annual variability, the 50th and 99th percentiles are estimated at a seasonal scale and averaged over the length of the hindcast to provide an empirical estimate of the expected typical and extreme conditions during the different seasons (i.e., winter: December, January, February, DJF; spring: March, April, May, MAM; summer: June, July, August; JJA; autumn: September, October, November, SON). The results presented for the four seasons show the regions of the basin where the largest values occur and those with the largest temporal variability.

Moreover, the Extreme Value Analysis (EVA) was performed on the model results to estimate the extreme events of a given probability or return period (e.g. 100-year event). The return period indicates the duration of time (typically years) which corresponds to the probability that a given value (e.g. wind speed) would be exceeded at least once within a year. This probability is called the probability of exceedance and is related to return periods as *1/p* where *p* is the return period. In common terminology, z_p is the return level associated with the return period *1/p*, since to a reasonable degree of accuracy, the level z_p is expected to be exceeded on average once every year. More precisely, z_p is exceeded by the annual maximum in any particular year with probability *p*. EVA was performed using the *pyextremes* Python package (https://georgebv.github.io/pyextremes/) with the Peaks Over Threshold method for selecting extreme events from time series and the Maximum Likelihood Estimate fitting approach assuming a generalised Pareto distribution.

4.1 Sea level climate

The characteristics of the Adriatic Sea sea level climate obtained from the CERRA wind-forced model hindcast are presented as the 1994-2019 50th (typical climate) and 99th (extreme climate) percentiles. The largest values of typical climate occur in the northern Adriatic Sea along the Italian coast, mostly due to the effect of the major Bora wind regime (Fig. 5a). The extreme climate shows a marked south-north gradient with the largest values in the northern Adriatic Sea and in the Gulf

of Trieste (Fig. 5b). This spatial distribution is due to the fact that the northern Adriatic Sea is characterized by the larger tidal range and storm surges components over the whole basin.

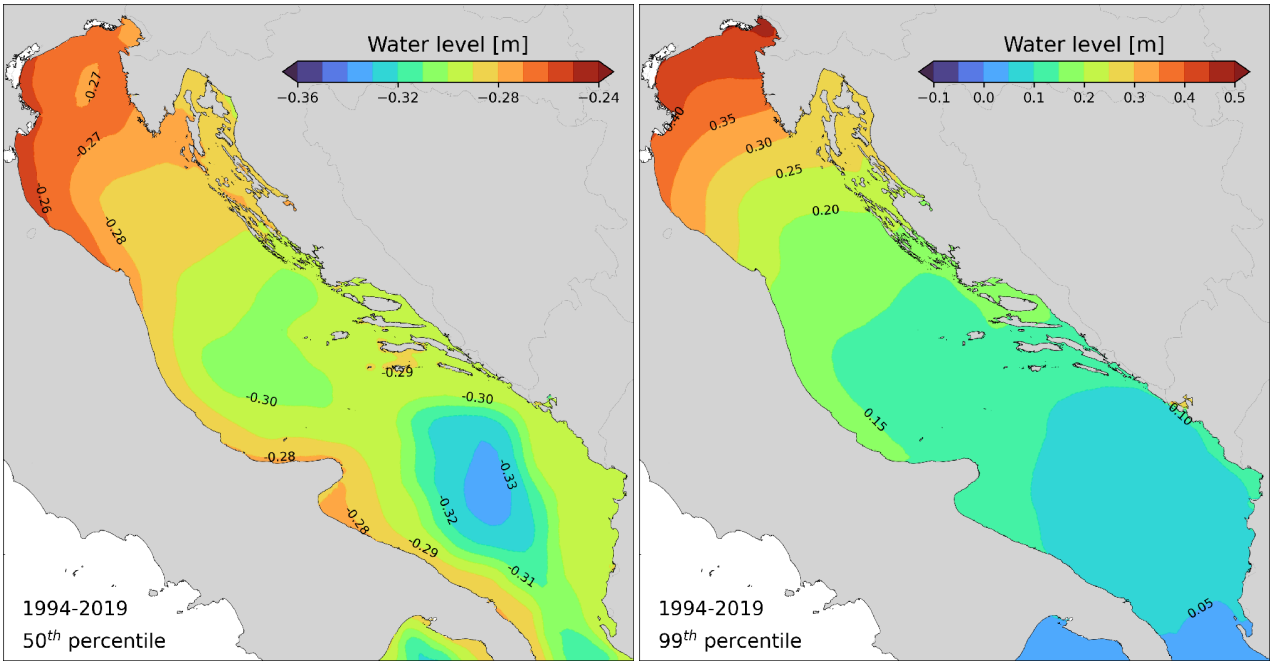

Fig. 5. 1994-2019 climate of the Adriatic sea levels as the 50th and 99th percentile maps.

The seasonal climate of the extreme values is reported in Fig. 6. As expected, the largest 99th percentile values occur during the winter (NDJ) season when wind speeds are typically stronger, while lower values are found in summer (JJA). Generally, the spatial patterns of the 99th percentile are similar in all seasons and characterized by a south-north gradient.

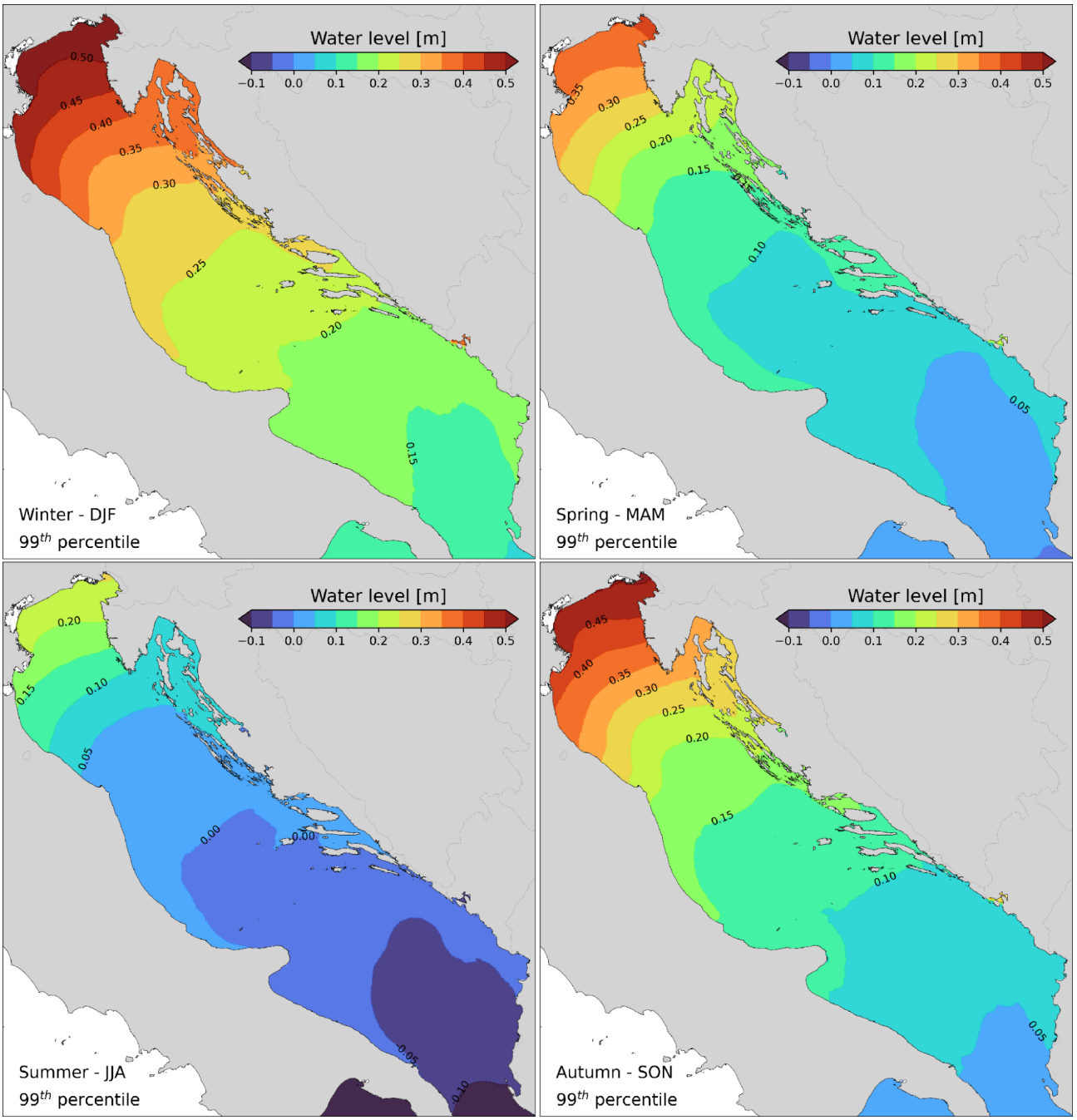

Fig. 6. Inter-annual variability of the extreme (99th percentile) sea level climate.

The water level values associated with return periods of 50 and 100 years are reported in Fig. 7. Similarly to the figure presented above, the return levels show a marked along-basin gradient with the largest values in the northern Adriatic Sea with peak values exceeding 1.4 m.

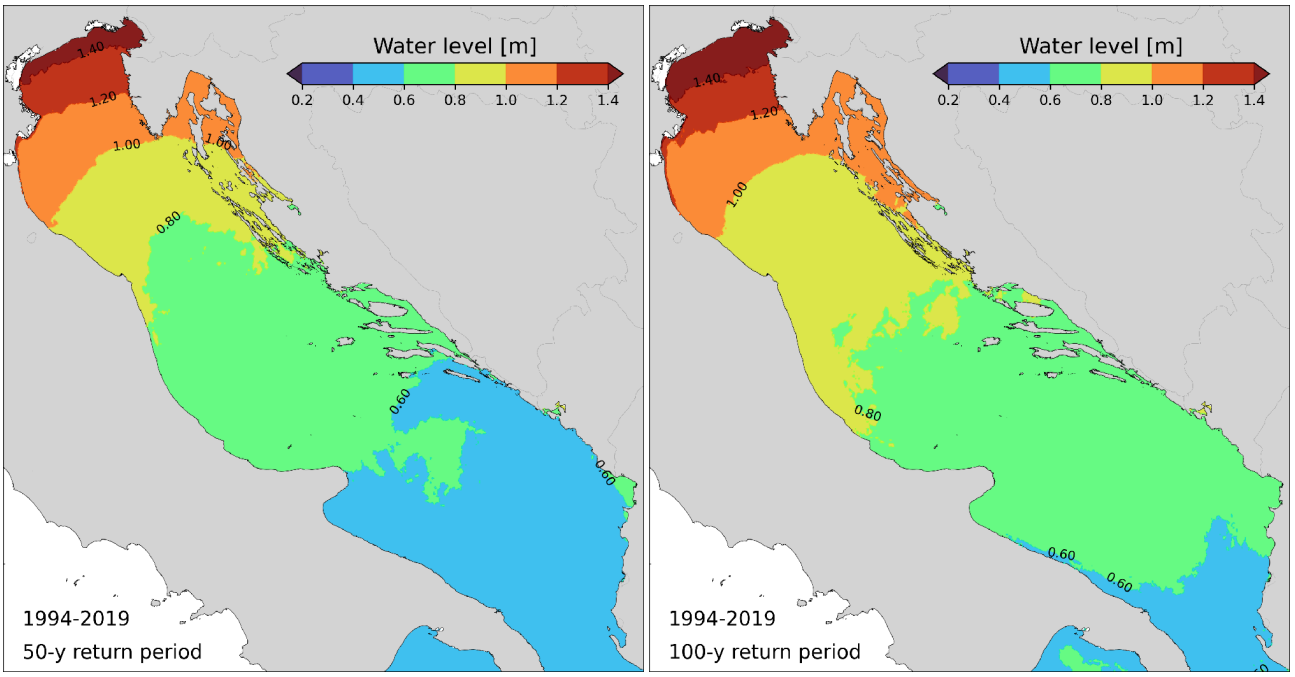

Fig. 7. Water level estimates for a return period of 50 and 100 years.

4.2 Significant wave height climate

The characteristics of the Adriatic Sea wind-wave climate obtained from the CERRA wind-forced WWM hindcast simulations are presented as the 50th and 99th percentiles of Hs. The typical and extreme Hs distributions are shown in Figure 8. The typical wave regime shows a north-south along-basin gradient. The largest waves are found in the southern Adriatic Sea with extreme values reaching more than 4 m.

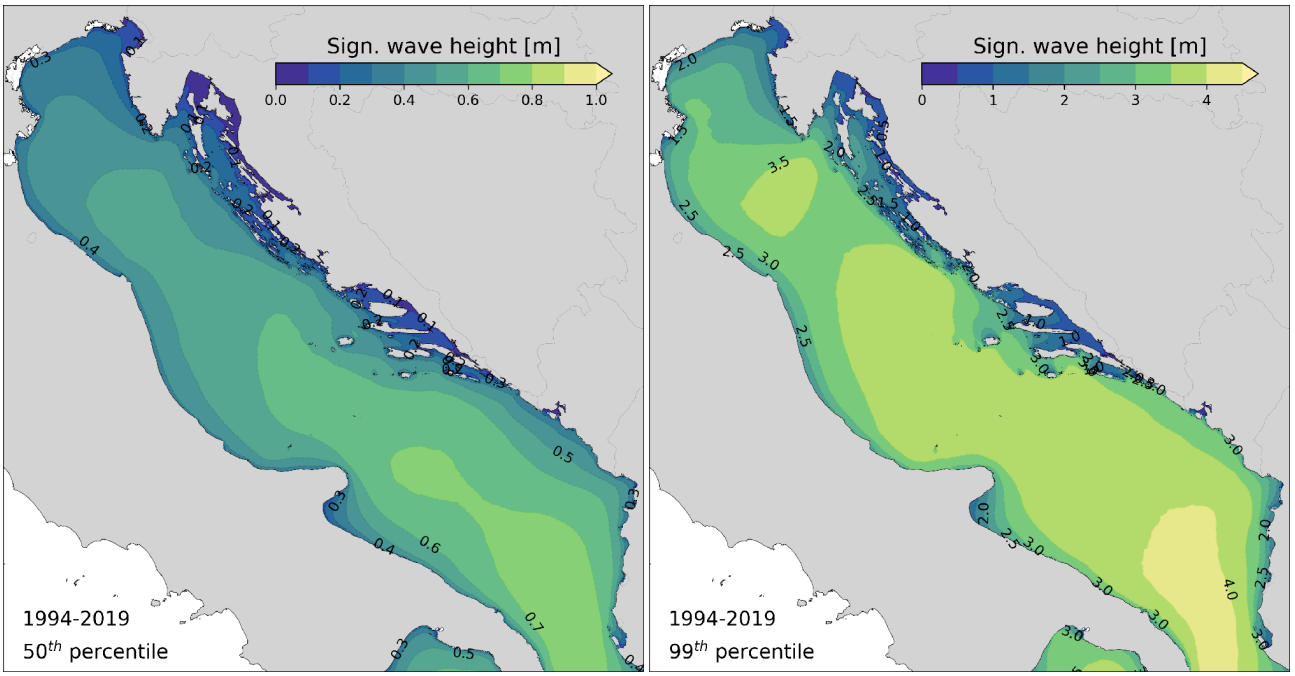

Fig. 8. 1994-2019 climate of the Adriatic significant wave height as the 50th and 99th percentile maps.

The seasonal climate of the extreme Hs values is reported in Fig. 9. As expected, the largest values occur during the winter (NDJ) season when wind speeds are typically stronger. Spatial patterns of the 99th percentile Hs are almost the same in the different seasons. The most energetic sea states occur over the southern sub-basin with values above 4 m in winter and autumn.

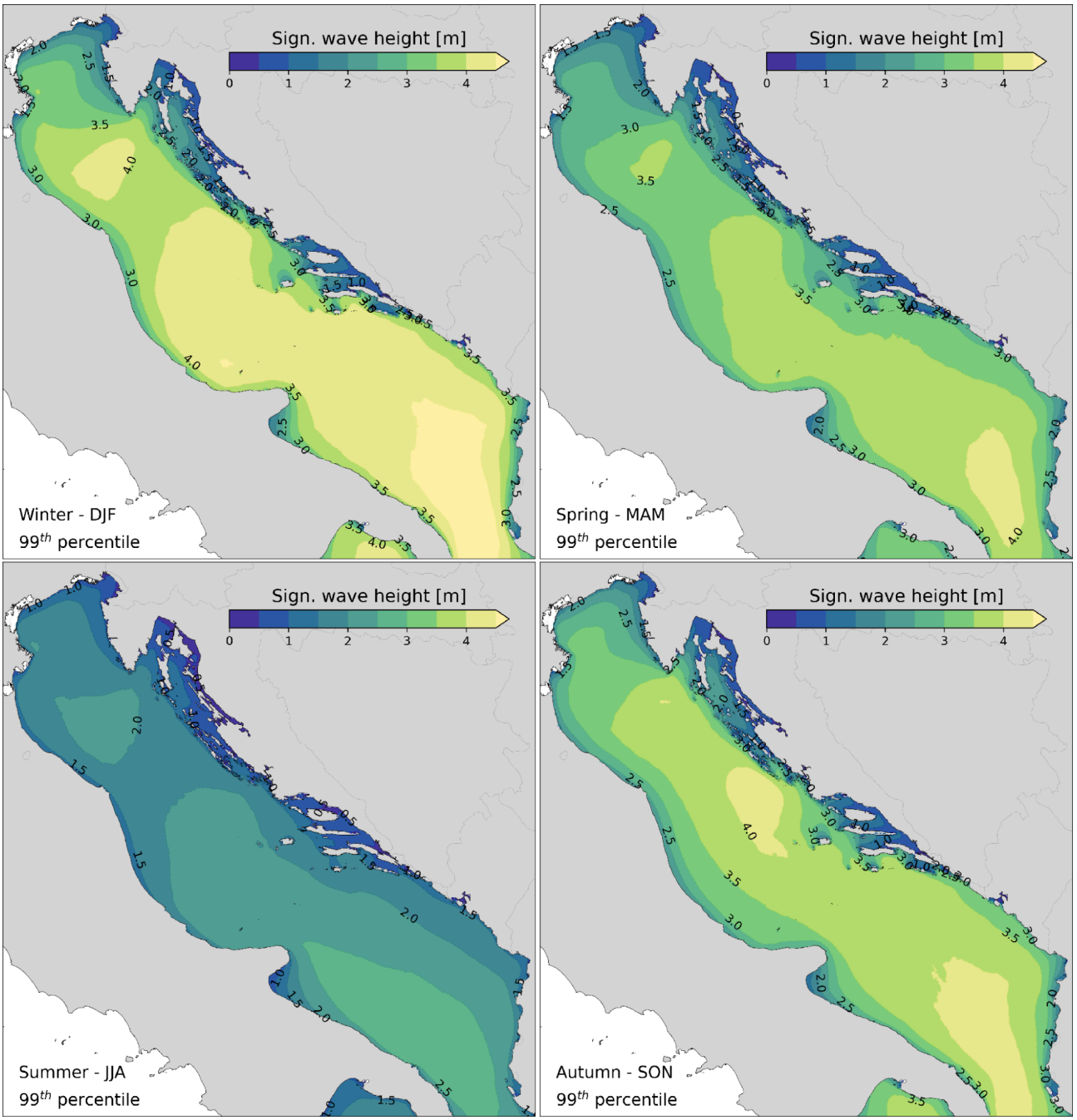

Fig. 9. Inter-annual variability of the extreme (99th percentile) significant wave height climate.

The significant wave height values associated with return periods of 50 and 100 years are reported in Fig. 10. Similarly to the figure presented above, the maximum Hs return levels are found in the southern part of the basin and in the coastal area in front of Rimini with values exceeding 8 m.

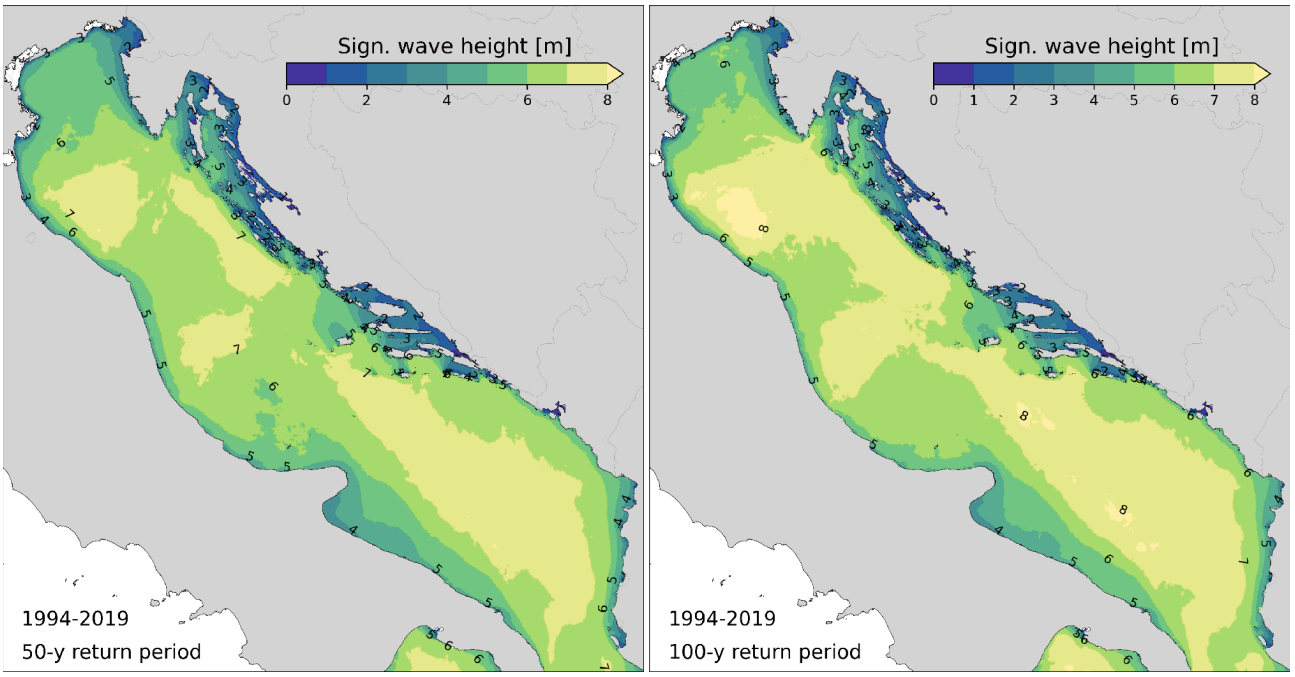

Fig. 10. Significant wave height estimates for a return period of 50 and 100 years.

5 COASTAL FLOOD HAZARD

In order to provide the perception of the physical processes acting along the Adriatic coastal areas that are responsible for storm-related flood hazards, the results of the models - in terms of sea level and wave conditions - were processed for different coastal segments. The coast is subdivided into segments of variable length in the function of morphology, human settlements and administrative boundaries. The coastal assessment units were selected according to the Mediterranean coastal database (MCD) developed by Wolff et al. (2018). The MCD segments have an average length of 4.5 km.

Over the whole Adriatic coastal region, the nearshore sea level and wave results provided by the models were combined with the coastal characteristics (coast material and slope) provided by the

MCD database for computing the coastal total water level (TWL), which should include the wave set-up and run-up. For the coastal segments characterised by sandy beaches, the TWL was computed by combining the sea level height, wave set-up and wave run-up according to Stockdon's formula (R_2, the 2 % exceedance level of run-up maxima; Stockdon et al., 2006). For gravel beaches and rocky cliffs, other methodologies should be used for estimating wave run-up (Dodet et al., 2018), but they could not be applied in this study due to the lack of the required detailed coastal information (sediment grain size, type of rocks, and permeability of the structure).

The 2% exceedance level of wave run-up maxima (R_2) computed according to Stockdon's formula, the simulated water levels and the total water levels associated with the 99th percentile are shown in Fig. 11.

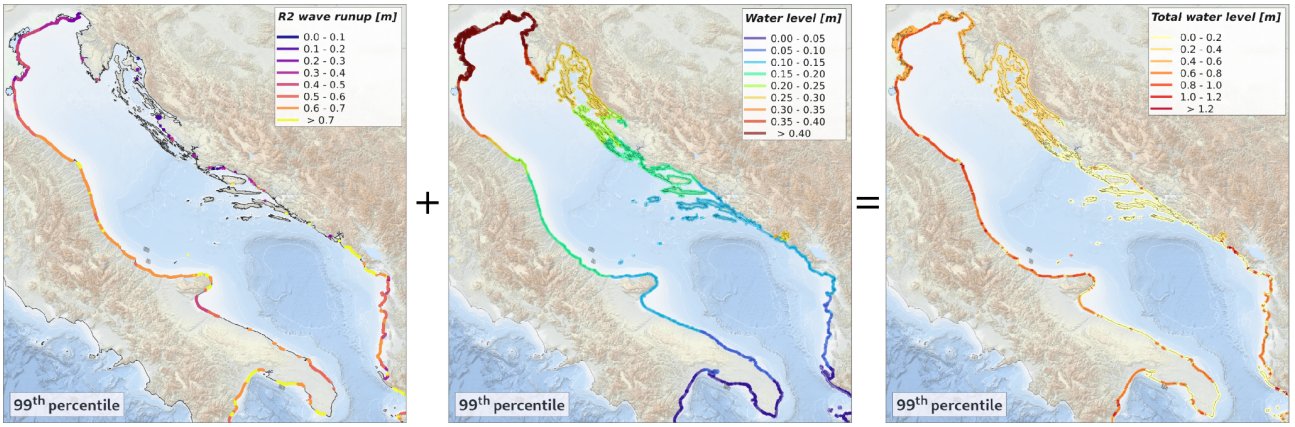

Fig. 11. R_2 wave runup, water level and total water level computed for the coastal segments along the Adriatic Sea.

Wave runup is computed mostly along the Italian and Albanian coasts where sandy beaches are located. The wave run-up estimation increases with the beach slope and therefore, the high wave run-up values found at some coastal segments (e.g. along the Marche, Abruzzo and Puglia regions) are due not only to the severe wave conditions but also to the fact that these areas are characterised by a steep coast (slope > 0.15). In such reflective conditions, the use of an alongshore-averaged beach slope in practical applications of the run-up parameterisation may result in large run-up errors (Stockdon et al., 2006). Wave runup estimation is added to the simulated 99th percentile water level to obtain the total water level at every considered coastal segment. TWL represents thus the flood hazard along the coast to be used in flood risk analysis.

6 REFERENCES

Bajo M., Međugorac, I., Umgiesser, G. and Orlić, M. Storm surge and seiche modelling in the Adriatic Sea and the impact of data assimilation, Quart. J. Roy. Meteor. Soc., 145, 2070-2084, doi: 10.1002/qj.3544, 2019.

Barbariol F., Davison S., Falcieri F.M., Ferretti R., Ricchi A., Sclavo M. and Benetazzo A. Wind Waves in the Mediterranean Sea: An ERA5 Reanalysis Wind-Based Climatology. Front. Mar. Sci. 8:760614. doi: 10.3389/fmars.2021.760614, 2021.

Barnard, P.L., Erikson, L.H., Foxgrover, A.C. et al. Dynamic flood modeling essential to assess the coastal impacts of climate change. Sci Rep 9, 4309, doi: 10.1038/s41598-019-40742-z, 2019.

Bellafiore, D., Mc Kiver, W., Ferrarin, C., Umgiesser, G. The importance of modeling nonhydrostatic processes for dense water reproduction in the southern Adriatic Sea. Ocean Model. 125, 22-28, doi: 10.1016/j.ocemod.2018.03.001, 2018.

Bertotti, L., Cavaleri, L. Wind and wave predictions in the Adriatic Sea. J. Marine Syst. 78 (Supplement), S227–S234, 2009.

Dodet, G., Leckler, F., Sous, D., Ardhuin, F., Filipot, J., and Suanez, S.: Wave Runup Over Steep Rocky Cliffs, J. Geophys. Res. Oceans, 123, 7185–7205, https://doi.org/10.1029/2018jc013967, 2018.

EMODnet Bathymetry Consortium: EMODnet Digital Bathymetry (DTM), https://doi.org/10.12770/bb6a87dd-e579-4036-abe1-e649cea9881a, 2020.

Ferrarin, C., Roland, A., Bajo, M., Umgiesser, G., Cucco, A., Davolio, S., Buzzi, A., Malguzzi, P., and Drofa, O.: Tide-surge-wave modelling and forecasting in the Mediterranean Sea with focus on the Italian coast, Ocean Model., 61, 38–48, https://doi.org/10.1016/j.ocemod.2012.10.003, 2013.

Ferrarin, C., Bellafiore, D., Sannino, G., Bajo, M., and Umgiesser, G.: Tidal dynamics in the inter-connected Mediterranean, Marmara, Black and Azov seas, Prog. Oceanogr., 161, 102–115, https://doi.org/10.1016/j.pocean.2018.02.006, 2018.

Ferrarin, C., Davolio, S., Bellafiore, D., Ghezzo, M., Maicu, F., Drofa, O., Umgiesser, G., Bajo, M., De Pascalis, F., Malguzzi, P., Zaggia, L., Lorenzetti, G., Manfè, G., and Mc Kiver, W.: Cross-scale operational oceanography in the Adriatic Sea, J. Oper. Oceanogr., 12, 86–103, https://doi.org/10.1080/1755876X.2019.1576275, 2019.

Ferrarin, C., Bajo, M., Benetazzo, A., Cavaleri, L., Chiggiato, J., Davison, S., Davolio, S., Lionello, P. Orlić, M., and Umgiesser, G.: Local and large-scale controls of the exceptional Venice floods of November 2019, Prog. Oceanogr., 197, 102628, https://doi.org/10.1016/j.pocean.2021.102628, 2021.

Hersbach, H, Bell, B, Berrisford, P, et al.: The ERA5 global reanalysis. Quart. J. Roy. Meteor. Soc. 146: 1999-2049, doi: 10.1002/qj.3803, 2020.

Kantha, L.H., 1995. Barotropic tides in the global oceans from a nonlinear tidal model assimilating altimetric tides 1. Model description and results. J. Geophys. Res.100 (C12), 25, pp. 283–25, 309.

Longuet-Higgins, M.S., Steward, R.W. Radiation stresses in water waves; a physical discussion with applications. Deep-Sea Res. 11, 529–562, 1964.

Schimanke S., Ridal M., Le Moigne P., Berggren L., Undén P., Randriamampianina R., Andrea U., Bazile E., Bertelsen A., Brousseau P., Dahlgren P., Edvinsson L., El Said A., Glinton M., Hopsch S., Isaksson L., Mladek R., Olsson E., Verrelle A., Wang Z.Q.: CERRA sub-daily regional reanalysis data for Europe on single levels from 1984 to present. Copernicus Climate Change Service (C3S) Climate Data Store (CDS), doi: 10.24381/cds.622a565a, 2021.

Sotillo, M.G., Cailleau, S., Lorente, P., Levier, B., Aznar, R., Reffray, G., Amo-Baladron, A., Chanut, J., Benkiran, M., Alvarez-Fanjul, E.: The MyOcean IBI Ocean Forecast and Reanalysis Systems: operational products and roadmap to the future Copernicus Service. J. Oper. Oceanogr. 8, 63–79. http://dx.doi.org/10.1080/1755876X.2015.1014663, 2015.

Stockdon, H. F., Holman, R. A., Howd, P. A., and Sallenger, A. H.: Empirical parameterization of setup, swash, and runup, Coast. Eng., 53, 573–588, https://doi.org/10.1016/j.coastaleng.2005.12.005, 2006.

Roland, A., Cucco, A., Ferrarin, C., Hsu, T.-W., Liau, J.-M., Ou, S.-H., Umgiesser, G., and Zanke, U.: On the development and verification of a 2d coupled wave-current model on unstructured meshes, J. Marine Syst., 78, Supplement, S244–S254, https://doi.org/10.1016/j.jmarsys.2009.01.026, 2009.

Umgiesser, G., Ferrarin, C., Cucco, A., De Pascalis, F., Bellafiore, D., Ghezzo, M., Bajo, M. Comparative hydrodynamics of 10 Mediterranean lagoons by means of numerical modeling. J. Geophys. Res. Oceans 119, 2212–2226, doi: 10.1002/2013JC009512, 2014.

Wolff, C., Vafeidis, A. T., Muis, S., Lincke, D., Satta, A., Lionello, P., Jimenez, J. A., Conte, D., and Hinkel, J.: A Mediterranean coastal database for assessing the impacts of sea-level rise and associated hazards, Sci. Data, 5, 180044, https://doi.org/10.1038/sdata.2018.44, 2018.

Xia, H., Xia, Z., Zhu, L. Vertical variation in radiation stress and wave-induced current. Coastal Eng. 51, 309–321, 2004.

Zou, Q.-P., Chen, Y., Cluckie, I., Hewston, R., Pan, S., Peng, Z. and Reeve, D. Ensemble prediction of coastal flood risk arising from overtopping by linking meteorological, ocean, coastal and surf zone models. Q.J.R. Meteorol. Soc., 139: 298-313, doi: 10.1002/qj.2078, 2013